

# Aromatic Copolyimide Membranes for High Temperature Gas Separations: $H_2/CH_4$ , $H_2/N_2$ , and $O_2/N_2$

H. C. W. M. BUYS, A. VAN ELVEN, A. E. JANSEN and  
A. H. A. TINNEMANS, *TNO Division of Technology for Society*,  
*P.O. Box 108, 3700 AC Zeist, The Netherlands*

## Synopsis

A series of high-molecular weight condensation polyimides prepared from pyromellitic dianhydride (PMDA) or 3,3,4,4'-benzophenone tetracarboxylic dianhydride (BTDA) with 4,4'-oxydianiline (ODA) and/or 1,5-diaminonaphthalene (NA), and a series of high-molecular weight condensation poly(amide-imides) prepared from trimellitic anhydride acid chloride (TMAC) with ODA and/or NA were evaluated to determine, in the temperature region 50–250°C, the effect of polymer molecular structure on the permeability and ideal permselectivity of hydrogen, oxygen, nitrogen, and methane. Replacement of ODA with NA generally decreases the permeability of each gas but it increases the permselectivity, which is explained by suppression of both the packing disruption effect and intrasegmental mobility of the amine segments. In general, the overall lower permeation values for the TMAC series of polyimides are much lower than the BTDA-derived series, being the highest for the PMDA-derived series. Permeation data were used to calculate the performance of a hollow fiber module on an industrial scale. It is shown that hydrogen can be efficiently recovered (> 90%) with a purity of at least 95% from ammonia synthesis off-gas with a feed concentration of 61 mol % of hydrogen.

## INTRODUCTION

Aromatic polyimides possess a number of physical properties that make them attractive candidates for membrane materials for gas separation: a high mechanical and thermal stability, a good resistance towards organic solvents, and a high permselectivity for small molecules compared to larger molecules.<sup>1–10</sup> The favorable gas separation properties may be ascribed to the fact that such glassy, amorphous polymers with a high glass-transition temperature could have intersegmental gap sizes between molecular aggregates, responsible for gas diffusion, in a very controlled order because of a small distribution of thermal segmental motions. Only a few studies have been done on the relationship between gas separation properties and chemical structure of polyimidic membranes.<sup>5–9</sup> It was shown in a series of polyimides derived from pyromellitic dianhydride (PMDA) and the aromatic diamines 4,4'-oxydianiline (ODA), 4,4'-methylenedianiline (MDA), and 4,4'-isopropylidenedianiline (IPDA) that the packing ability is an important factor to influence the permeation rate. As intersegmental packing is disrupted by bulky substituents, gas diffusivities are generally increased but diffusivity selectivities are correspondingly decreased.<sup>6,7</sup> However, simultaneous suppression of intrasegmental mobility and intersegmental packing yields a significant increase in permselectivity.<sup>8</sup>

The present study was undertaken to evaluate the effect of molecular structure of polyimidic backbone, containing both flexible and more stiff monomers, upon the transmission rates of H<sub>2</sub>, O<sub>2</sub>, N<sub>2</sub>, and CH<sub>4</sub> in the temperature region 50–250°C. The study was performed on solution-cast films that had systematic dianhydride and diamine changes. Particularly, the use of stiff 1,5-diaminonaphthalene is expected to reduce the intrasegmental chain-mobility by which jumping of molecules with a relatively large kinetic gas diameter such as N<sub>2</sub> and CH<sub>4</sub> is strongly prohibited.

## EXPERIMENTAL

### Materials

The solvents dimethylacetamide (DMAc), dimethylformamide (DMF), and N-methylpyrrolidone-2 (NMP) were purified by treatment with P<sub>2</sub>O<sub>5</sub> for 2–4 h at 160–190°C followed by distillation, under nitrogen atmosphere, over fresh P<sub>2</sub>O<sub>5</sub>. In order to maintain optimal purity, they were stored under nitrogen. Monomers obtained from Janssen Chimica, except PMDA from VEBA Chemie A.G., were purified by repeated crystallization: pyromellitic dianhydride (PMDA) and 3,3',4,4'-benzophenone tetracarboxylic dianhydride (BTDA) from acetic anhydride, trimellitic anhydride acid chloride (TMAC) from cyclohexane, 4,4'-oxydianiline (ODA) from n-butanol/chloroform 1/1 v/v, and 1,5-diaminonaphthalene (NA) from ethanol/H<sub>2</sub>O 10/1 v/v and ethanol. Polyamic acid precursors were prepared by solution condensation of an aromatic dianhydride with a stoichiometric amount of an aromatic diamine in DMF, according to standard procedures.<sup>11</sup>

The synthesis of poly(amide-amic acid) precursors was performed in an analogous way in the presence of four equivalents of pyridine as HCl binder. In a typical example, 8.42 g (0.04 mol) of TMAC was added over a 5 min period to a stirred solution of 3.16 g (0.02 mol) of NA and 4.00 g (0.02 mol) of ODA in 80 mL of DMAc. An exothermic reaction occurred by which the temperature rose to 50°C. After 15 min, 13 mL (0.16 mol) of purified dry pyridine was slowly added to the moderately viscous reaction mixture, and the mixture was heated at ca. 45°C for 16–20 h to achieve a complete reaction. The polymer was isolated by precipitation in water, by four times resuspension in water and once in acetone, washing with acetone, and drying in vacuo over P<sub>2</sub>O<sub>5</sub> at 40°C.

### Preparation of Films

In preparation for film casting, polyamic acid or the poly(amide-amic acid) solutions (6–20 wt %) were filtered using a metal chamber containing a glass matt filter (Schleicher and Schüll nr. 8) by applying a nitrogen head pressure of 100–200 kPa. The casting solution was kept overnight to minimize the inclusion of air bubbles. As the properties of a polyimide film may depend upon its imidization protocol,<sup>6</sup> a standard imidization procedure was applied for preparation of all samples. Films (150–250 μm) were cast from solution on a precleaned glass plate through the use of a doctor's blade. Films on glass plates were carefully evaporated for 1–2 h at 100°C in an oven without circulation, and, subsequently, for 16 h at 120°C in an oven under the flow of dry nitrogen.

TABLE I  
Solution and Film Properties of PMDA- and BTDA-Derived Polymers

Molar ratio				Polyamic acid $\eta_{inh}$ [1/g] <sup>a</sup>	Polyimide film	
					DMF <sup>b</sup> (wt %)	$\eta_{inh}$ [1/g] <sup>c</sup>
PMDA						
1		1		0.165	8.0	0.062
1		0.75	0.25	0.185	8.0	0.054
1		0.50	0.50	0.178	6.6	d
1		0.25	0.75	0.230	6.0	d
	1	1		0.082	10.4	d, e
	1	0.75	0.25	0.106	10.1	d, e
	1	0.50	0.50	0.079	10.2	d, e
	1	0.25	0.75	0.102	10.1	d, e

<sup>a</sup> Inherent viscosity (DMF, 25°C) as used for film casting.

<sup>b</sup> Casting solution of polyamic acid.

<sup>c</sup> H<sub>2</sub>SO<sub>4</sub> concd, 25°C.

<sup>d</sup> Brittle materials.

<sup>e</sup> Insoluble in concd H<sub>2</sub>SO<sub>4</sub>.

Then, each film was thermally imidized on the glass plate in a vacuum oven by heating one hour each at 150, 200, and 250°C, and finally 4 h at 300°C. Under these conditions the conversion of the amic acid to the imidized polyimide has been shown to be complete.<sup>12</sup> After cooling to below 25°C, the imidized film was removed from the glass plate by stripping in a water bath, and dried. The results are compiled in Tables I and II.

The copolyimides derived from PMDA and BTDA start to decompose at ca. 510°C, in agreement with a series of copolyimides based on PMDA/ODA/benzidine.<sup>12</sup> The polymers based on TMAC, however, have a decomposition temperature at 410°C.

TABLE II  
Solution and Film Properties of TMAC-Derived Polymers

Molar ratio				Poly(amide-amic acid) $\eta_{inh}$ [1/g] <sup>a</sup>	Poly(amide-imide) film	
					DMAc <sup>b</sup> (wt %)	$\eta_{inh}$ [1/g] <sup>c</sup>
TMAC						
1		1		0.077	20	0.098
1		0.75	0.25	0.086	15	0.080
1		0.50	0.50	0.092	11.1	0.079
1		0.25	0.75	0.110	15	0.091
1			1	0.099	15	0.077
0.75	0.25		1	0.075	15	0.080
0.50	0.50		1	0.075	15	0.075

<sup>a</sup> Inherent viscosity (NMP, 25°C) as used for film casting.

<sup>b</sup> Casting solution of poly(amide-amic acid).

<sup>c</sup> Concd H<sub>2</sub>SO<sub>4</sub>, 25°C.

### Equipment and Procedures

Inherent viscosities were measured in DMF or NMP as the solvent at a concentration of 5 g/L. In some cases the restricted solubility of the polymers only allowed measurements at 2 g/L. Thermal gravimetric analysis (TGA) experiments were performed using a DuPont-957 apparatus to examine the thermal properties of the imidized samples.

The experimental set-up for gas permeation is shown schematically in Figure 1. It is based on the apparatus described by Toi et al.<sup>13</sup> with minor modifications. A polyester plastic film was used as standard reference material (National Bureau of Standards, SRM 1470) to verify the measurements of the gas transmission rates which were accurate within 2%. Pure gas permeation data were recorded for H<sub>2</sub> up to 200 kPa and for the other gases up to 1 MPa in the temperature region 50–250°C. Permeabilities of H<sub>2</sub>, O<sub>2</sub>, and N<sub>2</sub> tended to be relatively independent of pressure, whereas those of CH<sub>4</sub> showed a very slight pressure dependence at elevated feed pressure, similar to earlier observations.<sup>14</sup>

### Scale-up Considerations

In order to get an indication of the performance of the copolyimide membranes in industrial applications, a computer model was developed which describes transport phenomena as a function of process conditions and membrane characteristics for the case of a hollow fiber module. This model is based on the mathematical algorithms formulated by Pan,<sup>16</sup> and is based on the following assumptions:

1. The feed gas is on the skin side of the asymmetric membrane.

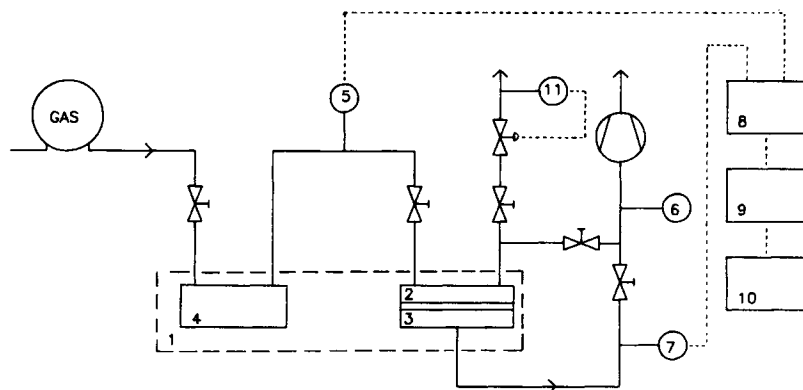


Fig. 1. Block diagram of permeation apparatus: (1) thermostatted oven ( $\pm 1$  K); permeation cell: permeation chamber (2) separated from retention chamber (3) by a 3 mm porous steel plate (Poral Innox) (4) buffer vessel; (5) Statham capacitive absolute pressure transmitter (PA2000-3000-01, range 0–6 MPa) for monitoring start signal; (6) Pirani gauge (range 0.1–10 Pa) for monitoring vacuum degree of system; (7) Rosemount capacitive absolute pressure transmitter (AP5E22, range 0–100 kPa) to measure the pressure change at the permeate side with the aid of a multimeter (8). This transmitter is externally triggered by a clock (9) HP Multiprogrammer 6942A. The process is controlled and evaluated by a HP 9000 computer (10). When the pressure rise in the time is linear ( $r > 0.9999$ ), the permeability is calculated from the pressure rise with the general gas law. (11) Mass flow control.

2. No mixing of permeate fluxes of different compositions occurs inside the porous supporting layer of the membrane.
3. The porous supporting layer has negligible resistance to gas flow, and diffusion along the pore path is insignificant due to high permeate flux.
4. The membrane permeabilities are independent of pressure and concentration.
5. Feed gas pressure drop is negligible.
6. The permeate flow inside the fiber is governed by the Hagen-Poiseuille equation. This is a reasonable assumption based on the analysis of laminar flow in a channel with porous walls.
7. The deformation of the fiber under pressure is assumed to be negligible.
8. The flow pattern is cocurrent.

The membrane/module dimensions are chosen to be: hollow fiber: effective length 1 m; outer diameter 300  $\mu\text{m}$ ; inner diameter: 100  $\mu\text{m}$ . Module: diameter 0.2 m; number of hollow fibers 87,300; effective surface of membranes 82  $\text{m}^2$ ; package density 2620  $\text{m}^2/\text{m}^3$ .

## RESULTS AND DISCUSSION

### Permeability and Permselectivity

From the permeation versus temperature data of the gases  $\text{H}_2$ ,  $\text{O}_2$ ,  $\text{N}_2$ , and  $\text{CH}_4$  for the various PMDA-, BTDA-, and TMAC-based polyimide films, Arrhenius plots can be derived showing straight lines with high correlation coefficients. A typical set is presented in Figures 2-4. The energies of activation for the permeation of  $\text{H}_2$ ,  $\text{O}_2$ ,  $\text{N}_2$ , and  $\text{CH}_4$  calculated from the slopes amount to 18.8, 23.0, 27.5, and 31.5  $\text{kJ mol}^{-1}$ , respectively, which values are in the same

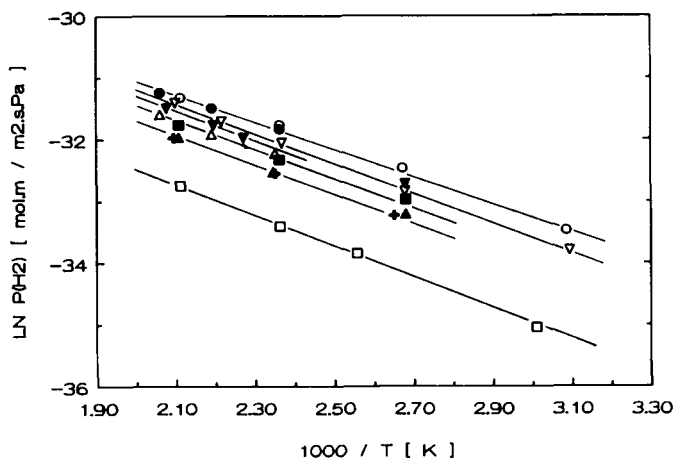


Fig. 2. Permeabilities of  $\text{H}_2$  for PMDA-ODA ( $\circ$ ), PMDA-ODA-NA (1/0.75/0.25) ( $\bullet$ ), BTDA-ODA ( $\nabla$ ), BTDA-ODA-NA (1/0.5/0.5) ( $\blacktriangledown$ ), TMAC-ODA ( $\square$ ), TMAC-ODA-NA (1/0.75/0.25) ( $\blacksquare$ ), TMAC-ODA-NA (1/0.25/0.75) ( $\blacktriangle$ ), TMAC-NA ( $+$ ), TMAC-BTDA-NA (0.75/0.25/1) ( $\triangle$ ) as a function of temperature.

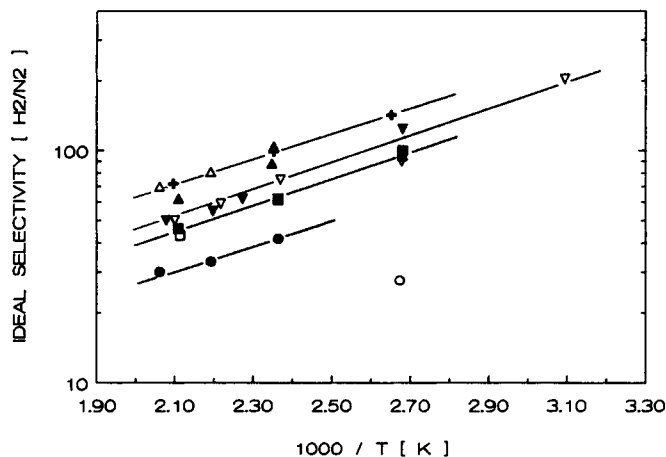


Fig. 3. Ideal selectivities,  $P(\text{H}_2)/P(\text{N}_2)$ , for various copolyimides as a function of temperature. For explanation of symbols, see Figure 2.

order of magnitude as the energies of activation for diffusion in amorphous polymers.<sup>15</sup>

To understand the permeability ( $P_i$ ) of gas component  $i$  and ideal permselectivity ( $P_i/P_j$ ) behaviour as related to the chemical structures of constituent polymers, it is assumed that the changes in  $P_i$  and  $P_i/P_j$  are primarily due to the changes in diffusivity factors. The solubility factors play a minor role, which is supported by the fact that the logarithm of the permeability of each gas studied is directly proportional to the kinetic gas diameter ( $\text{H}_2$ : 2.82 Å,  $\text{O}_2$ : 3.47 Å,  $\text{N}_2$ : 3.80 Å, and  $\text{CH}_4$ : 3.76 Å) for each temperature. According to Koros et al.<sup>7,8</sup> the diffusivity selectivity arises from the inherent ability of polymer matrices to function as size- and shape-selective media. This ability is primarily determined by such factors as polymer segmental mobility and intersegmental packing.

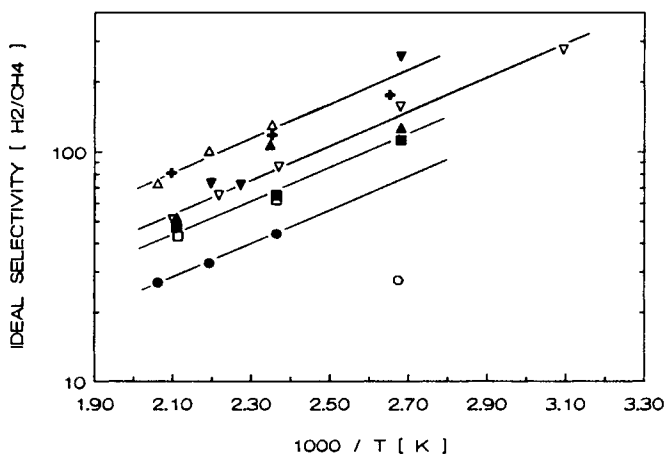


Fig. 4. Ideal selectivities,  $P(\text{H}_2)/P(\text{CH}_4)$ , for various copolyimides as a function of temperature. For explanation of symbols, see Figure 2.

The permeabilities of  $H_2$  for PMDA-ODA and BTDA-ODA amount to  $80.0 \times 10^{-16}$  and  $54.9 \times 10^{-16}$  mol m/m<sup>2</sup> s Pa at 100°C, respectively, in good agreement with literature data.<sup>9</sup> As the polymer is varied from PMDA-ODA to PMDA-ODA-NA (1/0.75/0.25), the permeability of  $N_2$  and  $CH_4$  is significantly decreased, whereas the permeability of  $H_2$  is not affected. Although the selectivities are rather low ( $P(H_2)/P_j = 27.6$ ), it is striking that replacement of ODA with a small percentage of NA (25 mol %) causes a two- and three-fold increase for  $P(H_2)/P(N_2)$  (= 58.5) and  $P(H_2)/P(CH_4)$  (= 73.2), respectively. Qualitatively, the same effects are observed as the polymer is varied from BTDA-ODA to BTDA-ODA-NA (1/0.5/0.5): a small decrease of the permeability of each gas and an increase in ideal permselectivity. This is explained as follows. As the PMDA segment in the PMDA-ODA materials is "packable" and rigid, whereas the ODA segment has a swivel point at the center, the presence of the ODA part of the repeat unit is believed to be primarily responsible for intrasegmental mobility and intersegmental disruption.<sup>7,8</sup> By the introduction of NA, however, both the packing disruption effect and the intrasegmental mobility of the amine segments are decreased due to the rigid nature of NA. Obviously, these effects are most explicitly seen from the reduction of the permeabilities of molecules with a relatively large kinetic diameter.

In order to get better permselectivities, we have made attempts to build in higher amounts of NA in both PMDA-ODA and BTDA-ODA. Unfortunately, the films obtained after imidization were too brittle to be evaluated.

Comparison of the permeation data for corresponding PMDA- and BTDA-polyimide films indicates that BTDA-based films have lower permeabilities for  $H_2$ ,  $N_2$ , and  $CH_4$ , and a higher selectivity for  $P(H_2)/P(N_2)$  and  $P(H_2)/P(CH_4)$ .<sup>9</sup> This phenomenon, observed earlier too for  $O_2$  and  $CO_2$ ,<sup>5</sup> suggests a higher packing ability of the BTDA-based films despite an extra swivel point in the BTDA segment. It is more likely, however, that other chemical factors, such as crosslinking during the imidization reaction, may have a significant effect since films, based on merely BTDA as dianhydride component, are, after imidization, insoluble in concentrated sulphuric acid.

TMAC-based films containing both amide and imide linkages between segmental units exhibit much lower permeabilities of  $H_2$  than the corresponding PMDA- and BTDA-based films containing merely imide linkages between segmental units. For instance, the permeability of  $H_2$  at 100°C, being  $80.0 \times 10^{-16}$  mol m/m<sup>2</sup> s Pa for PMDA-ODA, drops dramatically in the case of TMAC-ODA, viz.,  $14.1 \times 10^{-16}$  mol m/m<sup>2</sup> s Pa. This implies a general increase in packing ability of TMAC segments which may be due to the formation of intermolecular hydrogen bonds between amide bonds. This formation of hydrogen bonds is partly disrupted by partial replacement of ODA by 25 mol % NA, and leads to a considerably increased permeability of  $H_2$ , viz.  $47.9 \times 10^{-16}$  mol m/m<sup>2</sup> s Pa. Qualitatively, the same effects are observed for the permeabilities of both  $N_2$  and  $CH_4$ . However, upon introduction of a much higher amount of NA, the packing disruption effect and the intrasegmental mobility are again suppressed as seen in the PMDA and BTDA series. As a result of the increased packing density, the permeability of all gases studied for TMAC-ODA-NA (1/0.25/0.75) and TMAC-ODA is decreased, being  $38.1 \times 10^{-16}$  and  $34.5 \times 10^{-16}$  mol m/m<sup>2</sup> s Pa at 100°C, respectively, for  $H_2$ . The higher permselectivities for  $H_2/N_2$  and  $H_2/CH_4$  gas pairs are also consistent with the fact that the structural

change by introduction of 75–100 mol % NA is more effective for the molecules with a relatively large kinetic gas diameter.

Introduction of more imidic segments, as the polymer is varied from TMAC–NA to TMAC–BTDA–NA (0.75/0.25/1), provides an even looser packing tendency, resulting in an increase of the permeation rates of each gas while maintaining the permselectivity.

As seen from Figure 5, the permeation rates of  $O_2$  for the copolyimides investigated are very low. For instance, for PMDA–ODA the permeability of  $O_2$  amounts to  $0.8 \times 10^{-16}$  mol  $m/m^2$  s Pa at  $100^\circ\text{C}$  which is, after extrapolation to  $25^\circ\text{C}$  using the  $E_a$  value of  $23.0$  kJ  $\text{mol}^{-1}$ , in the same order of magnitude as the value reported by Sykes and St. Clair.<sup>5</sup> On partial replacement of ODA by 25 mol % NA, the permeability decreases, due to a decrease of the packing disruption effect and intrasegmental mobility of the amine segments, as explained above. Further, for the TMAC-based poly(amide-imide) films, it is found that the higher the amount of NA built into the polymer backbone, the lower the permeabilities of both  $O_2$  and  $N_2$ . As the NA content increases, the decrease of permeability is more pronounced for nitrogen, resulting in an increase of the permeability ratio  $P(O_2)/P(N_2)$ , being 8–10 at  $25^\circ\text{C}$  for TMAC/NA, TMAC/ODA/NA (1/0.25/0.75) and TMAC/BTDA/NA (0.75/0.25/1) (see Fig. 6).

### Application for $H_2$ Recovery

One of the copolyimide materials, TMAC–BTDA–NA (0.75/0.25/1), has been converted into an asymmetric membrane with an efficient thickness of the top layer equal to  $0.8$   $\mu\text{m}$ . From this result, it is concluded that the copolyimides are applicable in a gas separation module in an asymmetric form. Based on commercial data sheets from Monsanto and Ube Industries, the efficiency of a hollow fiber module, utilizing asymmetric membranes for ammonia synthesis off-gas, should meet the following requirements: a hydrogen recovery of at least 90% with a purity of at least 95%.

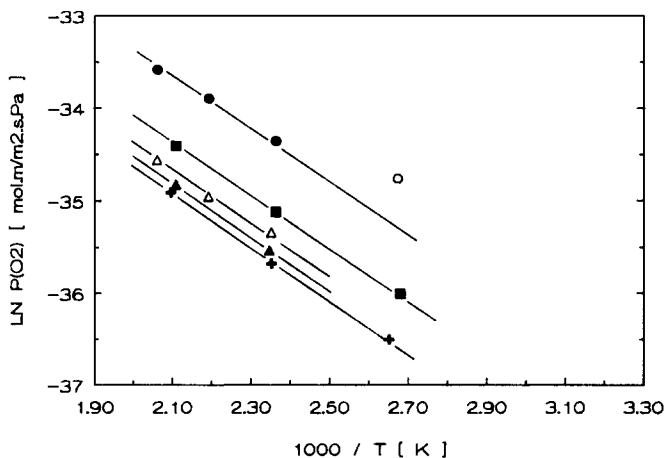


Fig. 5. Permeabilities of  $O_2$  for various copolyimides as a function of temperature. For explanation of symbols, see Figure 2.



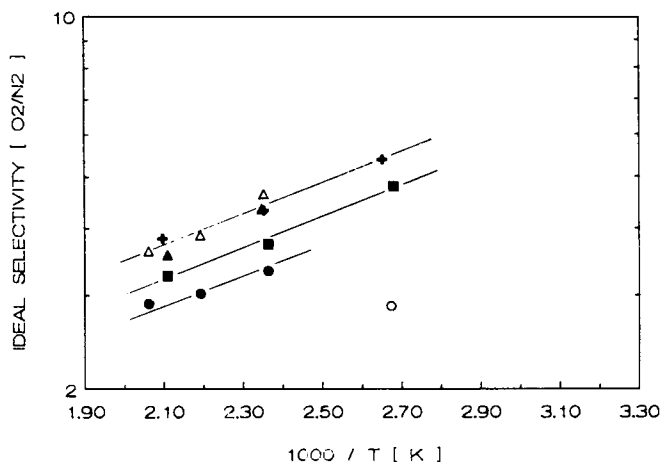


Fig. 6. Ideal selectivities,  $P(O_2)/P(N_2)$ , for various copolyimides as a function of temperature. For explanation of symbols, see Figure 2.

From the permeability data of a flat film of the copoly (amide-imide) above, we have calculated the efficiency of a hollow fiber module for ammonia synthesis off-gas using the scale-up considerations above. The process simulation is based on the following process conditions: feed concentration 61 mol %  $H_2$ , retentate pressure 14.2 MPa, permeate pressure 3 MPa.

In Figure 7 the hydrogen recovery efficiencies and feed flows are depicted as a function of temperature for permeate concentrations of hydrogen (95 and 99 mol %) and for various top layer thicknesses (0.1 and 1.0  $\mu\text{m}$ ). It is seen that it is feasible to increase the rate of hydrogen recovery 130-fold with a purity of 95% by raising the temperature from 25°C to 240°C, albeit with a concomitant loss of  $H_2$  from 7 to 28% or 18%, using a separation layer of 0.1 and 1.0  $\mu\text{m}$ ,

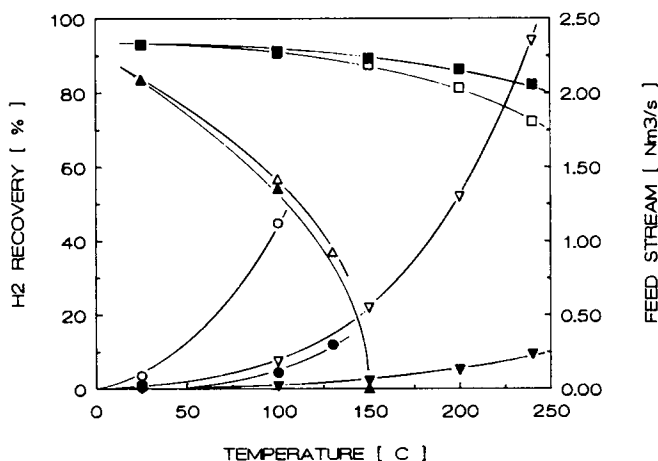


Fig. 7. Hydrogen recovery efficiencies [ $\square$ ,  $\blacksquare$ ] purity 95%; ( $\Delta$ ,  $\blacktriangle$ ) purity 99%] and feed flows ( $\nabla$ ,  $\blacktriangledown$ , resp.  $\circ$ ,  $\bullet$ ) from ammonia synthesis off-gas at various temperatures. Top layer thickness 0.1  $\mu\text{m}$  (open symbols) and 1.0  $\mu\text{m}$  (closed symbols).

respectively. Furthermore, a hydrogen recovery of 90% with a purity of 95% can be reached at temperatures up to 120°C and 150°C for a top layer of 0.1 and 1.0  $\mu\text{m}$ , respectively. For hydrogen recovery with a purity of 99%, however, the recovery, being 84% at 25°C, sharply drops at elevated temperatures. For instance, at 100°C or 150°C, the recovery values with a membrane of 0.1  $\mu\text{m}$  are 54 and 0.15%, respectively.

Analogous calculations performed for the recovery of  $\text{H}_2$  from a mixture of hydrogen/methane have shown that the separation of methane is slightly more effective than that of mixtures of hydrogen/nitrogen. With a top layer of 0.1  $\mu\text{m}$ , hydrogen recovery with a purity of 99% is feasible, albeit with a poor recovery efficiency (75% at 100°C and 35% at 150°C).

This investigation was carried out with support of the Dutch National Innovation Oriented Program Membrane Technology (IOP-m). The technical assistance of Mr. H. A. Budding for the preparation of the various types of poly (amide-imide) films is gratefully acknowledged.

### References

1. R. T. Chern, W. J. Koros, H. B. Hopfenberg, and V. T. Stannett, *Mater. Sci. Synth. Membr. Am. Chem. Soc. Symp. Ser.*, **269**, 25 (1985).
2. W. J. Koros, B. J. Story, S. M. Jordon, K. O'Brien, and G. R. Husk, *Polym. Eng. Sci.*, **27**, 603 (1987).
3. T. H. Kim, W. J. Koros, G. R. Husk, and K. O'Brien, *J. Appl. Polym. Sci.*, **34**, 1767 (1987).
4. M. Moe, W. J. Koros, H. H. Hoehn, and G. R. Husk, *J. Appl. Polym. Sci.*, **36**, 1833 (1988).
5. G. F. Sykes and A. K. St. Clair, *J. Appl. Polym. Sci.*, **32**, 3725 (1986).
6. K. C. O'Brien, W. J. Koros, and G. R. Husk, *J. Membr. Sci.*, **35**, 217 (1988).
7. T. H. Kim, W. J. Koros, G. R. Husk, and K. O'Brien, *J. Membr. Sci.*, **37**, 45 (1988).
8. T. H. Kim, W. J. Koros, and G. R. Husk, *Sep. Sci. Technol.*, **23**, 1611 (1988).
9. A. Nakamura, Y. Kusuki, T. Harada, K. Nakagawa, and M. Kinouchi, *Book of Abstracts of the 1987 International Congress on Membranes and Membrane Processes*, June 1987, Tokyo, p. 560.
10. K. Haraya, K. Obata, N. Itoh, Y. Shndo, T. Hakuta, and H. Yoshitome, *J. Membr. Sci.*, **41**, 23 (1989).
11. C. E. Sroog, A. L. Endrey, S. V. Abramo, C. E. Berr, W. M. Edwards, and K. L. Olivier, *J. Polym. Sci. A*, **3**, 1373 (1965).
12. C. P. Yang and S. H. Hsiao, *J. Appl. Polym. Sci.*, **31**, 979 (1986).
13. K. Toi, T. Ito, T. Shirakawa, H. Ichimura, and I. Ikemoto, *J. Appl. Polym. Sci.*, **29**, 2413 (1984).
14. E. Sada, H. Kumazawa, P. Xu, and M. Nishigaki, *J. Membr. Sci.*, **37**, 165 (1988).
15. J. Crank and G. S. Parks, *Diffusion in Polymers*, Academic, London, 1968.
16. C. Y. Pan, *Am. Soc. Chem. Eng.*, **29**, 540 (1983).
17. H. H. Hoehn, *Mater. Sci. Synth. Membr. Am. Chem. Soc. Symp. Ser.*, **269**, 81 (1985).

Received August 2, 1989

Accepted January 29, 1990